

Hollow core photonic crystal fiber as a reusable Raman biosensor

Altaf Khetani,^{1,*} Jason Riordon,² Vidhu Tiwari,¹ Ali Momenpour,¹ Michel Godin,² and Hanan Anis¹

¹School of Electrical Engineering and Computer Science (EECS), University of Ottawa, Ottawa, ON K1N 6N5, Canada

²Department of Physics, University of Ottawa, Ottawa, ON K1N 6N5, Canada

*altafkhetani@gmail.com

Abstract: We report that a single hollow core photonic crystal fiber (HC-PCF) can be used for repetitive characterization of multiple samples by Raman spectroscopy. This was achieved by integrating the HC-PCF to a differential pressure system that allowed effective filling, draining and refilling of samples into a HC-PCF under identical optical conditions. Consequently, high-quality and reliable spectral data could be obtained which were suitable for multivariate analysis (partial least squares). With the present scheme, we were able to accurately predict different concentrations of heparin and adenosine in serum. Thus the detection scheme as presented here paves a path for the inclusion of HC-PCFs in point-of-care technologies and environmental monitoring where rapid sample characterization is of utmost importance.

©2013 Optical Society of America

OCIS codes: (280.4788) Optical sensing and sensors; (060.5295) Photonic crystal fibers; (170.5660) Raman spectroscopy.

References and links

1. W. Urbanczyk, T. Martynkien, M. Szpulak, G. Statkiewicz, J. Olszewski, and J. Wojcik, "Photonic crystal fibers for sensing applications," Proc. SPIE **5950**, 260–269 (2005).
2. S. Arismar Cerqueira, Jr., "Recent progress and novel applications of photonic crystal fibers," Rep. Prog. Phys. **73**(2), 024401 (2010).
3. F. Benabid, F. Couny, J. C. Knight, T. A. Birks, and P. St. J. Russell, "Compact, stable and efficient all-fibre gas cells using hollow-core photonic crystal fibres," Nature **434**(7032), 488–491 (2005).
4. S. Smolka, M. Barth, and O. Benson, "Highly efficient fluorescence sensing with hollow core photonic crystal fibers," Opt. Express **15**(20), 12783–12791 (2007).
5. S. O. Konorov, C. J. Addison, H. G. Schulze, R. F. B. Turner, and M. W. Blades, "Hollow-core photonic crystal fiber-optic probes for Raman spectroscopy," Opt. Lett. **31**(12), 1911–1913 (2006).
6. F. Benabid, J. C. Knight, G. Antonopoulos, and P. St. J. Russell, "Stimulated Raman Scattering in Hydrogen-Filled Hollow-Core Photonic Crystal Fiber," Science **298**(5592), 399–402 (2002).
7. X. Yang, C. Shi, R. Newhouse, J. Z. Zhang, and C. Gu, "Hollow core photonic crystal fibers for surface-enhanced Raman scattering probes," Int. J. Opt. **2011**, 754610 (2011).
8. Y. Han, S. L. Tan, M. K. K. Oo, D. Pristinski, S. Sukhishvili, and H. Du, "Towards full-length accumulative surface-enhanced Raman scattering-active photonic crystal fibers," Adv. Mater. **22**(24), 2647–2651 (2010).
9. Y. Zhang, C. Shi, C. Gu, L. Seballos, and J. Z. Zhang, "Liquid core photonic crystal fiber sensor based on surface enhanced Raman scattering," Appl. Phys. Lett. **90**(19), 193504 (2007).
10. F. M. Cox, A. Argyros, M. C. J. Large, and S. Kalluri, "Surface enhanced Raman scattering in a hollow core microstructured optical fiber," Opt. Express **15**(21), 13675–13681 (2007).
11. F. Eftekhari, J. Irizar, L. Hulbert, and A. S. Helmy, "A comparative study of Raman enhancement in capillaries," J. Appl. Phys. **109**(11), 113104 (2011).
12. G. O. S. Williams, J. S. Chen, T. G. Euser, P. S. Russell, and A. C. Jones, "Photonic crystal fibre as an optofluidic reactor for the measurement of photochemical kinetics with sub-picomole sensitivity," Lab Chip **12**(18), 3356–3361 (2012).
13. A. Khetani, M. Naji, N. Lagali, R. Munger, and H. Anis, "A method for using Photonic Crystal Fiber as a Raman biosensor" US Patent 2010/0014077 (2010).
14. V. S. Tiwari, A. Khetani, M. Naji, and H. Anis, "Study of Surface Enhanced Raman Scattering (SERS) within Hollow Core Photonic Crystal Fiber," IEEE Sensors **5404**, 367–370 (2009).

15. A. Khetani, V. S. Tiwari, A. Harb, and H. Anis, "Monitoring of heparin concentration in serum by Raman spectroscopy within hollow core photonic crystal fiber," *Opt. Express* **19**(16), 15244–15254 (2011).
16. V. S. Tiwari, A. Khetani, A. Momenpour, B. Smith, H. Anis, and V. L. Trudeau, "Detection of amino acid neurotransmitters by surface enhanced Raman scattering and hollow core photonic crystal fiber," *Proc. SPIE* **8233**(82330Q), 82330Q (2012).
17. J. Riordon, M. Mirzaei, and M. Godin, "Microfluidic cell volume sensor with tunable sensitivity," *Lab Chip* **12**(17), 3016–3019 (2012).
18. C. Schaschke, "Fluid Mechanics: Worked Example for Engineers Chapter 3" Rugby, Warwickshire, UK: IChemE. (2005).
19. Polymicro Technologies catalog, "Estimating the Flow Rate in Capillary: Flow Rate in Capillaries" http://www.exploreourcapabilities.com/catalog/3_10.htm accessed February 24, 2013.
20. G. W. Kaye and T. H. Laby, *Viscosities Tables of physical and chemical constants* (Harlow, Essex: Longman 1999) Chap. 2.
21. K. H. Esbensen, *An introduction to multivariate data analysis and experimental design* (Camo Inc. Oslo 2004).
22. C. M. McGoverin, A. S. S. Clark, S. E. Holroyd, and K. C. Gordon, "Raman spectroscopic quantification of milk powder constituents," *Anal. Chim. Acta* **673**(1), 26–32 (2010).
23. D. L. Johnston, P. D. Scanlon, D. O. Hodge, R. B. Glynn, J. C. Hung, and R. J. Gibbons, "Pulmonary function monitoring during adenosine myocardial perfusion scintigraphy in patients with chronic obstructive pulmonary disease," *Mayo Clin. Proc.* **74**(4), 339–346 (1999).
24. J. W. Chen, X. P. Liu, K. J. Feng, Y. Liang, J. H. Jiang, G. L. Shen, and R. Q. Yu, "Detection of adenosine using surface-enhanced Raman scattering based on structure-switching signaling aptamer," *Biosens. Bioelectron.* **24**(1), 66–71 (2008).

1. Introduction

Hollow core photonic crystal fibers (HC-PCF) are gaining importance as optical sensing devices [1–3]. These fibers have hollow core and cladding microchannels which can be filled with fluidic samples. In recent years, several publications have highlighted the use of HC-PCFs with various kinds of spectroscopic techniques such as fluorescence, Raman spectroscopy, surface enhanced Raman scattering (SERS), evanescent-field absorption, etc [4–11]. The majority of these reports are dedicated to the use of HC-PCFs for Raman spectroscopy. They provide insight into the methods of filling the HC-PCF waveguides with fluidic samples and ways to collect their Raman spectrum [10,11]. HC-PCFs can be used as nanolitre sample containers, and are therefore ideal for characterizing low-volume chemical and biological samples. They can also enhance the Raman signal of a sample by supporting strong light-matter interactions due to their photonic band gap. To this end, researchers have selected an excitation wavelength that overlaps with the transmission band of the sample-filled HC-PCF to achieve higher detection sensitivities for molecules [12–14].

Even though the role of HC-PCFs as a 'Raman signal enhancer' has been well established, the question remains whether they possess the necessary attributes for real world sensing applications. The practical difficulties associated with implementing HC-PCFs for real-time monitoring of samples are as follows: first, light coupling and guidance are affected by the frequent formation of air gaps or discontinuities in sample distribution within the microchannels. This results in poor quality spectra that do not correlate well with chemical concentration. Second, HC-PCFs are typically used once and replaced. Replacement of the HC-PCF is not only time-consuming but also influences the light coupling conditions. Variability in the light launching conditions from one HC-PCF to another alters the propagation properties making it difficult to ensure spectral reproducibility which is a key requirement for statistical analysis. Finally, HC-PCF-based sensors are traditionally filled through capillary action, a slow technique incapable of meeting the high-throughput demands of clinical instrumentation.

In an effort to solve these challenges, we present a novel detection scheme that uses Raman spectroscopy for monitoring samples filled into a HC-PCF using an integrated pressure-driven flow system. To demonstrate the device's detection capabilities, we measured various concentrations of both aqueous ethanol and isopropanol, followed by different concentrations of heparin and adenosine in serum. The sensor's fluidic architecture includes two bypass channels on both ends of the HC-PCF laid out in an H-configuration. The HC-

PCF was perpendicularly connected to the bypass channels and the sample flow is controlled by applying a pressure gradient. The HC-PCF integrated with a pressure-driven flow control system enabled rapid injection and draining of sample solutions into its channels. This design configuration offers a high degree of control and reproducibility on the sample flow rate and direction, which facilitates the multivariate analysis on the spectral data obtained from the sample filled into HC-PCF for quantitative analysis.

This paper builds on our previous work on HC-PCF-based Raman sensing and demonstrates the integration of a fluidic control system aimed at ensuring repeatability and reusability of the HC-PCF sensor [15,16]. We begin with a brief description of HC-PCF and propose a layout of an H-shaped differential pressure system common to microelectromechanical systems (MEMS) microfluidic flow control [17]. A discussion on the flow dynamics through the HC-PCF follows as it relates to the proposed differential pressure system. The device's performance was benchmarked using ethanol. Subsequent sections summarize our findings on optimal pressure difference, sample filling time into HC-PCF, and stability tests. We then applied the multivariate calibration model for accurately predicting the sensor's response to other chemicals such as ethanol, isopropanol, heparin and adenosine.

2. Experimental

2.1 Theory of HC-PCF

The light guiding properties of a non-selectively filled HC-PCF depends on the refractive index of the fluid sample. In this case, light is still guided using the bandgap but the transmission band supported by the fiber is shifted. The details of choosing the fiber depends on the wavelength and refractive index of the liquid sample, as previously described [15]. In this study, an excitation wavelength of 785nm was chosen with a HC-1550-04 hollow core photonic bandgap fiber (NKT Photonics). The fiber had a core size of 10.6 μm (+/-1 μm) and cladding channel diameter of 3.0 μm (+/-0.1 μm).

2.2 Sample Preparation

The ethanol and isopropanol were purchased from Commercial Alcohol and Fisher Scientific Ltd, respectively. Different concentrations of ethanol and isopropanol were independently prepared in deionized water in the concentration range of 5% to 60%. HyClone Bovine Calf Serum was purchased from Thermo Scientific Ltd. Adenosine was purchased from Lancaster Synthesis and a 50mM solution was prepared. Five concentrations of adenosine ranging from 5mM to 40mM were prepared in serum for recording Raman spectra using the HC-PCF sensor. MiniHep was purchased from Leo Pharmaceuticals in a vial of 25000 USP/ml concentrations. USP stands for United States Pharmacopeia (USP) and describes the potency of the drug in clinical applications. We then prepared seven concentrations of heparin in serum ranging from 25USP/ml to 1000USP/ml.

2.3 Flow dynamics

In each experiment, the HC-PCF sensor was filled with a fluidic sample and the corresponding Raman spectra was recorded at equilibrium. The HC-PCF was always rinsed with deionized water before and after the introduction of a new sample.

In order to estimate flow rates, we considered the flow of the sample through the microchannels as it displaced water. The flow rate (F) can be modeled using a modified Hagen-Poiseuille equation [18,19].

$$F = \frac{\pi r^4}{8\mu} \frac{\Delta P}{l} \quad (1)$$

where r is the channel radius, l the channel length, ΔP the pressure difference across the HC-PCF and μ the sample's viscosity. In this case, the viscosity will be continuously changing as

one sample flows through and replaces the first. We therefore introduce an average viscosity (μ_{avg}):

$$\mu_{avg} = \frac{\mu_{ethanol} + \mu_{water}}{2} \quad (2)$$

2.4 Experimental configuration

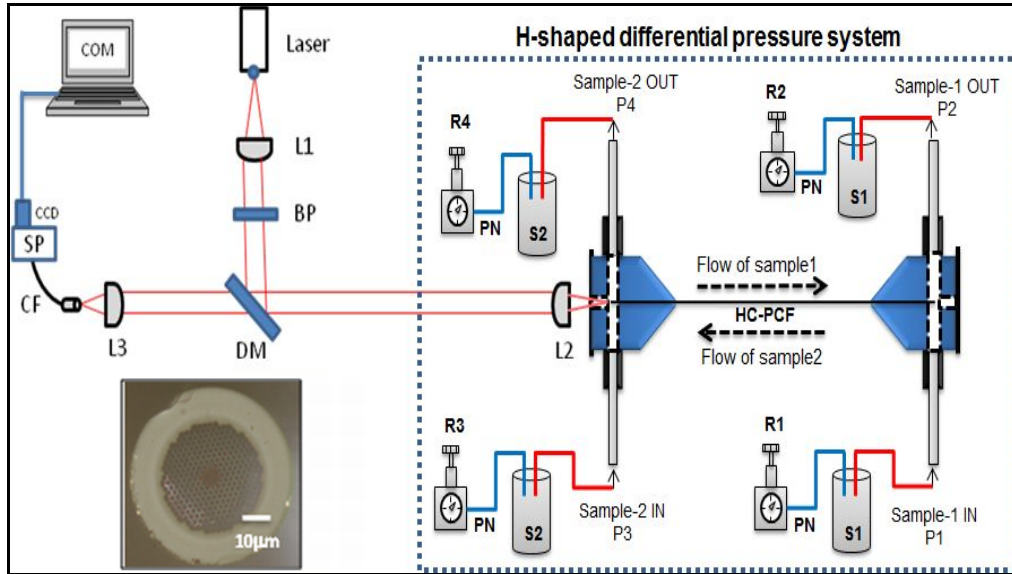


Fig. 1. Setup schematic. Laser: Laser source; L1: Collimating lens; BP: Band pass filter; DM: Dichroic Mirror; L2: Microscope objective lens for light coupling; H-shaped differential pressure system with hollow core photonic crystal fiber (HC-PCF); S1, S2: Samples in the vials; PN: Pressurized nitrogen R1-R4: Pressure regulators; L3: Microscope objective lens for backward light collection; CF: Collection fiber; SP: spectrograph; CCD: CCD camera; COM: Computer.

The layout of the HC-PCF sensor is shown in Fig. 1. It consisted of an optical Raman system and an H-shaped differential pressure system. The optical assembly employed a single mode 100mW, 14-pin butterfly pin laser (Photonic Solutions) with a central wavelength of 785nm. The beam was first sent through a bandpass filter (BP) centered at 785nm ($\pm 2\text{nm}$). It was directed through a dichroic filter (R785RDC, Chroma Technologies Corp.) which reflected 785nm ($\pm 5\text{nm}$) at an angle of 45° and transmitted a wide 790-1000 nm band. The dichroic filter acted as a reflector for the laser beam which was further focused onto the tip of the HC-PCF by a 40X microscope objective lens (L1) with numerical aperture (NA) of ~ 0.22 . Furthermore, the dichroic filter acted as a high pass filter for the back-scattered light from the sample-filled HC-PCF, thus allowing only the Raman wavelength to pass. The filtered Raman light was then imaged onto a fiber bundle (Fiberoptic System Inc., 26 multimode fiber, NA = 0.22) by another 6.3X microscope objective lens (L2) with a NA of ~ 0.22 . The output of the fiber bundle was interfaced into a Kaiser f/18i Spectrograph with a TE-cooled Andor CCD camera. The Andor SOLIS software was used for spectral data acquisition.

The other segment of the sensor configuration comprised of two parallel bypass flow channels: one for the input/output of the interrogated samples and the other for the purging fluid (water) input/output. Tubing leading in to each end of the bypass channel was immersed in the media (sample/purging liquid-water) contained in a glass vial. The other ends were connected to empty vials for collecting waste. Each vial was pressurized at different pressures P_1 , P_2 , P_3 and P_4 to control flow rates and directions, as shown in Fig. 1. The HC-PCF of

length 10cm was connected perpendicularly to each of these bypass channels via a customized 4-way microfluidic cross and mounted on a flexure stage (Thorlabs). The microfluidic cross was modified by removing one of its arm and by covering it with a glass cover slip to form an optical window for launching laser light. The fiber tip is inserted to the center of each device, exposing it to a strong perpendicular fluid flow. In preliminary testing, we found it advantageous for refilling to keep the fiber entrance at the center of this high-flow region, rather than near the chamber edge where flow is slower.

The integration of the HC-PCF perpendicularly with two parallel fluidic channels formed an H-shaped structure as shown in Fig. 1. In order to introduce sample 1 (sample mixture of interest) to the fiber channels, the average pressure of P_1 and P_2 was kept higher than that of P_3 and P_4 and for sample 2 (water) the pressure were reversed. The P_1 , P_2 , P_3 , P_4 values were varied to control flow rate and flow direction of the samples into HC-PCF.

3. Results and discussion

3.1 HC-PCF filling under different pressures

A fast sensor response time is desirable for practical applications. With this consideration, we first investigated the effect of the pressure difference (across HC-PCF) on the time to completely load the sample into the HC-PCF. The sample filling time was determined by tracking the Raman signal as it reached maximum (equilibrium) from zero (baseline). Figure 2 shows that the experimentally determined HC-PCF filling time is inversely proportional to the pressure difference across the fiber in the range of 15 to 60psi. At 60psi, the sample filling time was reduced to approximately 4min. It is to be noted that the maximum allowable pressure difference across the HC-PCF was limited by the pressure rating of the microfluidic cross fitting which was around 60psi. Equation (1) allowed us to estimate the sample flow rate in the microchannels of the HC-PCF. The viscosity of ethanol and water used to estimate the sample flow rate in HC-PCF with length 10cm were 1.09, and 1.00 centipoise (cP) respectively at 20°C [20]. As we have multiple channels in the fiber (see inset of Fig. 1), the flow rate is limited by the smallest channels in the fiber which are those of the cladding and have diameters of 3.0 μ m (+/- 0.1 μ m). Sample filling times (t) corresponding to various pressure differences (ΔP) were deduced from the calculated flow rates. Our experimentally determined sample filling times are consistent with predictions, as shown in Fig. 2

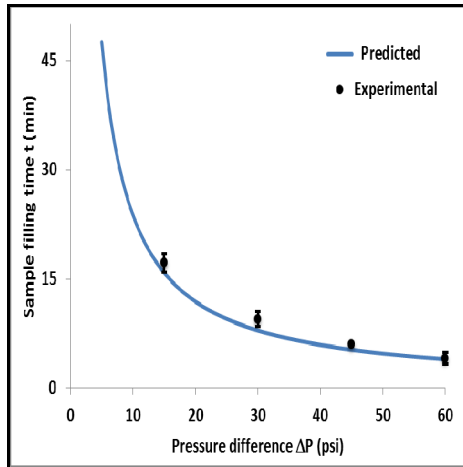


Fig. 2. Experimental and predicted sample filling times for different pressure differences across the HC-PCF (values used to estimate the filling times are microchannel radius - 1.5 μ m, length of the fiber - 10cm, viscosity of ethanol and water- 1.09, and 1.00 centipoise(cP) respectively at 20°C [20]).

3.2 Sample filling and Raman data

During this experiment, P_1 , P_2 , P_3 and P_4 were maintained at 62, 60, 2 and 0 psi, respectively. The Raman spectrum of the sample was recorded in time interval of 1min with an integration time of 0.5s when ethanol was introduced to the HC-PCF.

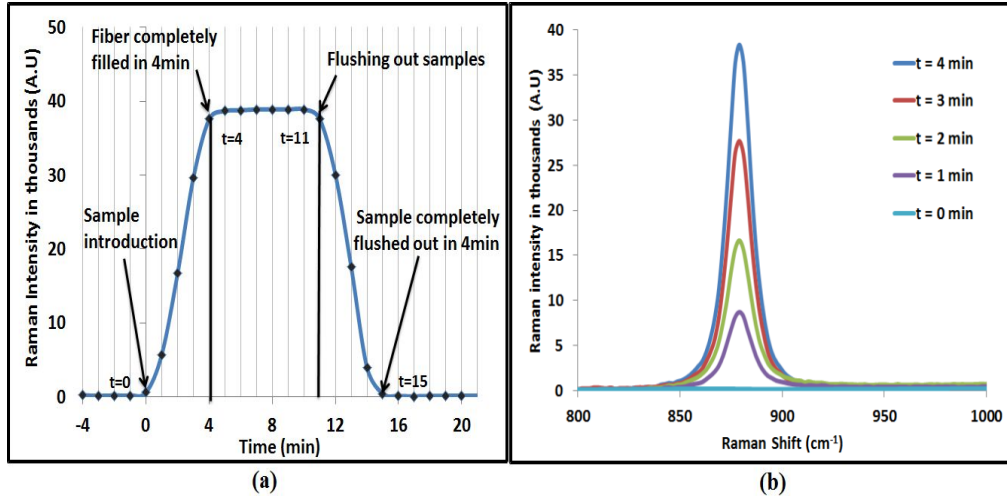


Fig. 3. (a) Filling HC-PCF with ethanol and flushing out ethanol (cycle) with time and (b) increase in the Raman signal of the ethanol solution as it filled the microchannels of the HC-PCF

The Raman peak at $\sim 880\text{ cm}^{-1}$ (C-C-O band) was monitored to track the sample filling time inside the HC-PCF. Figure 3(a) shows a complete fill/flush cycle. The experiment started by recording Raman spectra of the HC-PCF filled with water to obtain a baseline. At $t = 0\text{ min}$, ethanol sample was introduced into the HC-PCF by reversing the pressure across HC-PCF. This resulted in a gradual increase of the Raman peak intensity for ethanol as the sample mixtures entered the HC-PCF. At $t = 4\text{ min}$, the signal equilibrated indicating the complete filling of the fiber. At $t = 11\text{ min}$, the pressure difference across the HC-PCF was reversed to rinse the fiber channels with water. With the introduction of water a gradual decrease of the Raman peak for ethanol was observed which confirmed that water started displacing the ethanol from the other end while pushing the sample mixture out of the HC-PCF. The time required to completely purge the sample solution from the HC-PCF was found to be 4 mins as evidenced by the complete attenuation of the Raman peak of ethanol around 880 cm^{-1} at $t = 15\text{ min}$. Figure 3(b) shows the Raman peak of ethanol increased with time as it was seeping inside the microchannels of HC-PCF.

3.3 Repeatability and stability tests

The experimental procedure involved repeatedly filling the HC-PCF with fresh sample solution followed by purging the system with water. We made sure to completely remove the sample solution by displacing it with water prior to the injection of another sample. To assess reproducibility, 9 cycles were measured under identical experimental conditions. The Raman signal was monitored in each of these cycles and found to be almost identical as shown in Fig. 4(a). The Raman signal-to-noise ratio for the band located at 880 cm^{-1} was averaged around ~ 40000 with a deviation of 3%. Figure 4(b) illustrates reproducibility as multiple cycles of filling using the same sample was performed using the fluidic control system. These results suggest that the filling and flushing times are consistent from one experiment to another. This reproducibility demonstrates that integrating the HC-PCF to a differential pressure system allows the sensor to be reused by introducing different samples sequentially.

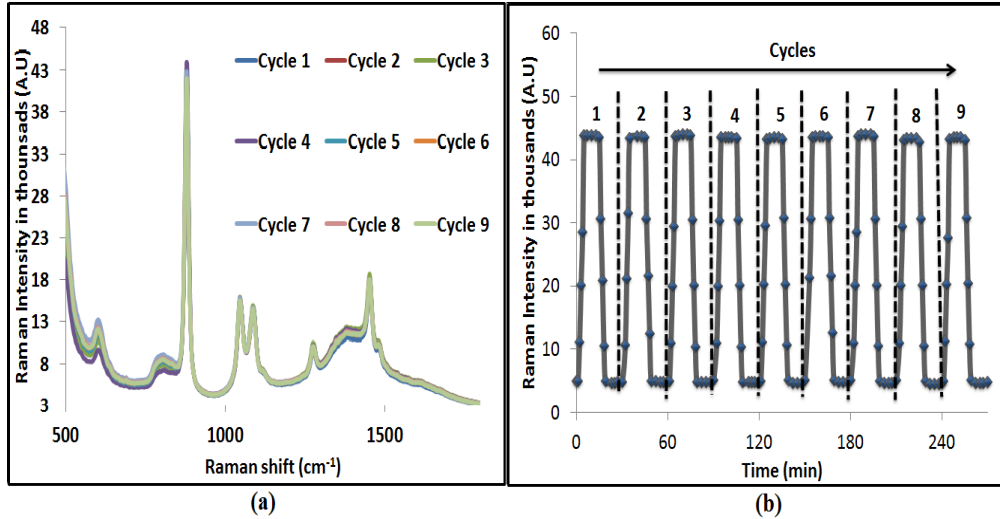


Fig. 4. (a) Raman signal of HC-PCF filled with 50% ethanol concentration (b) cycle of filling and flushing out sample

3.4 H-design HC-PCF for different concentration and PLS

The next phase of investigation focused on applying partial least square (PLS) analysis-an important multivariate chemometric method- on the Raman spectrum of various samples that were injected into the HC-PCF. A typical Raman spectrum includes noise. Multivariate techniques such as PLS minimizes the unwanted information (noise) from the Raman spectrum and thus establishes a direct correlation of Raman signal with sample concentration. The PLS performs the quantitative analysis of spectral data by constructing models where the response Y-variable (analytical data) depends on more than one explanatory X-variable (Raman shift wave number). During the formulation of the calibration model, linear combinations of only those explanatory X-variables are considered that are related to the response Y-variable. In the context of Raman spectroscopy, PLS is important as Raman bands are usually weak and overlapped: in which case, simple calibration curve between Raman signal intensity and sample concentration can give erroneous results [21].

The PLS has been widely used with Raman spectroscopy for trace level detection of bulk samples (cuvette) [22]. However, its application on the Raman spectral data as collected from the sample filled HC-PCF has not been reported to date. Conventionally, different HC-PCFs are employed for different sample sets. However, replicating the exact light coupling condition for every single HC-PCF is difficult as different modes are excited depending on the alignment of HC-PCF tip with respect to the focusing optics. Moreover, sample filling into the HC-PCF by capillary action, as practiced commonly, may not ensure complete filling of core and cladding channels, or the sample distribution may vary from one HC-PCF to another. As a result, light guidance within HC-PCF gets severely affected while the spectral background fluctuates from one spectrum to another. In such situations, any kind of multivariate analysis tool, including PLS, fails to establish a proper correlation of Raman signal to the species concentration which ultimately leads to an inability of predicting the sample constituents.

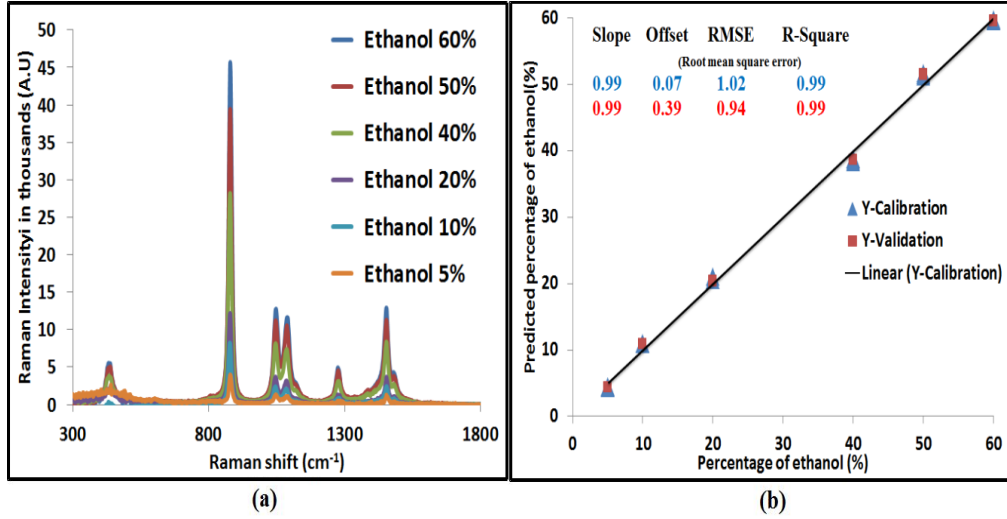


Fig. 5. (a) Raman spectra of different concentration of ethanol filled in a HC-PCF (b) PLS prediction

We injected different sample solutions into a single HC-PCF and recorded their respective Raman spectrum, without altering the light coupling condition. Between the consecutive injections of any two sample solution, we rinsed the HC-PCF with water to completely remove the traces of the preceding sample solution, ensuring high quality Raman spectra. The high quality spectral data set exhibited little spectral background fluctuation and was therefore suitable for direct multivariate analysis without requiring spectral pre-processing. Figure 5(a) shows the Raman spectrum of different sample solutions where the ethanol concentration varied with respect to water. PLS was applied to the spectral data to obtain a calibration curve as shown in Fig. 5(b). The calibration model predicts the concentration of ethanol in the range of 5-60% with a low root mean square of ~0.9%. The coefficient of determination (R^2) was found to be ~0.997 which indicated that the Raman spectral data of different ethanol-water samples correlated well with the concentration of ethanol. To further demonstrate our sensor's capabilities, we filled the HCPCF with various concentrations of isopropanol in water and recorded their respective Raman spectra. We then applied multivariate analysis for predicting the concentration of isopropanol. We found that the calibration model predicted accurately the isopropanol concentration with a low root mean square of ~0.1% and R^2 of ~0.997 as represented in Fig. 6(b).

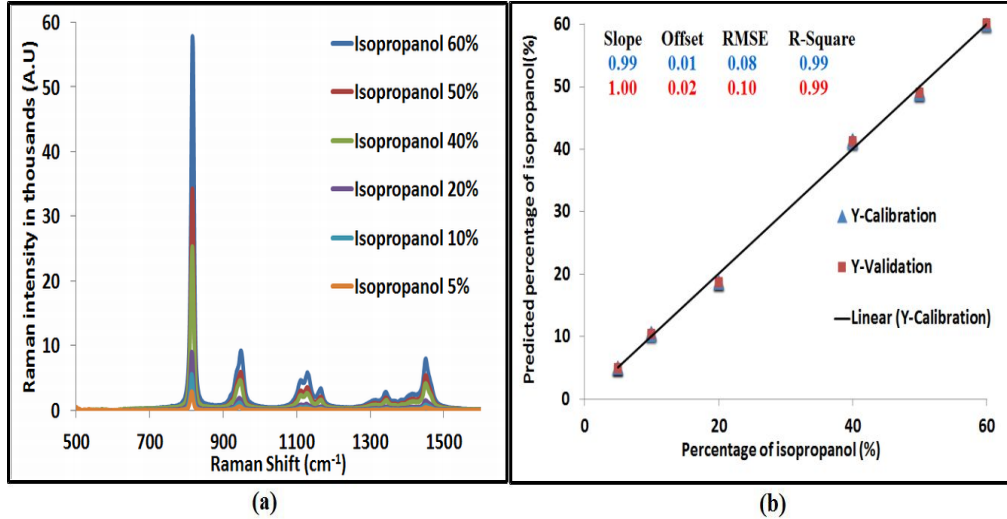


Fig. 6. (a) Raman spectra of different concentration of isopropanol filled in a HC-PCF (b) PLS prediction

3.5 HC-PCF for monitoring clinically important molecules

In the final stage of investigation, we inserted different samples of clinical importance such as heparin and adenosine in the HC-PCF with the pressure-driven flow system. Heparin is a clinically important blood anticoagulant which is commonly administered in a patient's blood during heart surgeries. In order to apply multivariate analysis on spectral data, we prepared seven different concentrations of heparin in serum in the range of 25USP/ml-1000USP/ml. We then recorded the Raman spectra for each concentration of heparin-serum mixtures.

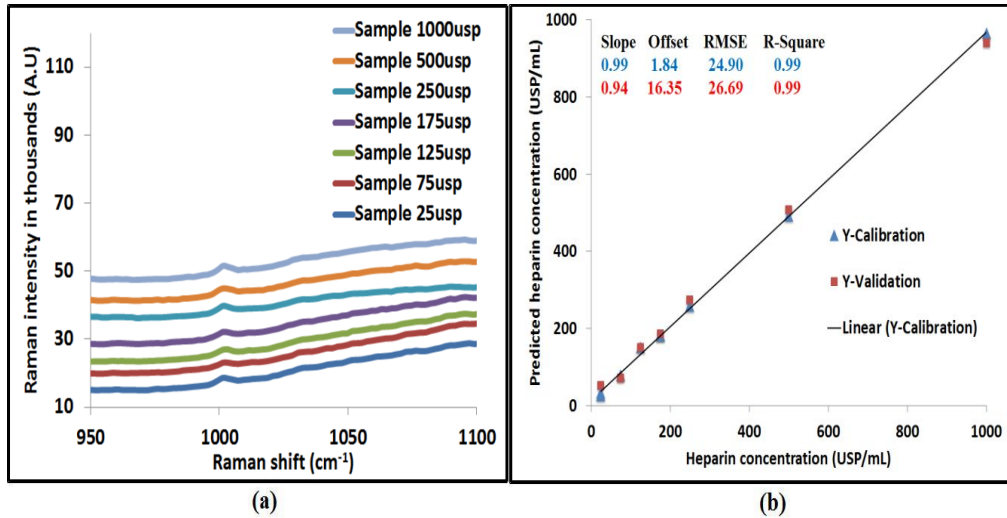


Fig. 7. (a) Raman spectra of different concentrations of heparin in serum filled in a HC-PCF (b) PLS prediction

Figure 7(a) shows the Raman spectra for heparin diluted in serum at different concentrations in the spectral range 950-1100 cm^{-1} . It is clear that Raman spectrums were overlapped and exhibited weak intensity of Raman peaks of heparin, hence no explicit correlation existed between Raman spectrum and concentrations. Under this situation, correlating the Raman bands of heparin with its concentration was very difficult by merely

formulating a simple calibration model. Hence, multivariate analysis (partial least squares analysis) was applied to the spectral data to infer the concentration of heparin in serum. Figure 7(b) shows the calibration curve with multivariate analysis. Compared to the results of the previous setup where there was no pressure differential system attached to HC-PCF (data not shown here), the coefficient of determination (R^2) was improved from 0.771 to 0.993 and root mean square error (RMSE) was reduced from 832 to 26 USP/ml.

The second clinically relevant molecule tested was adenosine. Adenosine is an important molecule in clinical environments as it regulates extra-cellular physiological activity. Monitoring adenosine is of vital importance due to its impact on pro-inflammatory and tissue destruction during bronchoconstriction in patients with asthma and chronic obstructive pulmonary disease (COPD) [23]. Sample solutions of adenosine in serum were prepared in the range of 5–40 mM. We recorded Raman spectra for adenosine diluted in serum at different concentrations as shown in Fig. 8(a). Adenosine exhibited a weak Raman peak at 724cm^{-1} due to the C_5N_7 vibrational mode as reported by Chen *et al.* [24]. A medium intensity Raman peak around 1000 cm^{-1} correspond to serum (Phenylalanine, C-C stretching) decreased as the adenosine concentration increased with respect to serum concentration. As in the case of heparin monitoring in serum, no direct correlation existed between Raman peak of adenosine and its concentration. Therefore, we applied PLS to infer the concentration of adenosine in serum, Fig. 8(b) shows the PLS-calibration curve with a R^2 of ~0.995 and RMSE of ~1.5%. These results indicate that the HC-PCF interfaced to pressure-driven flow system can be used as a biosensor to monitor clinically important molecules accurately and consistently.

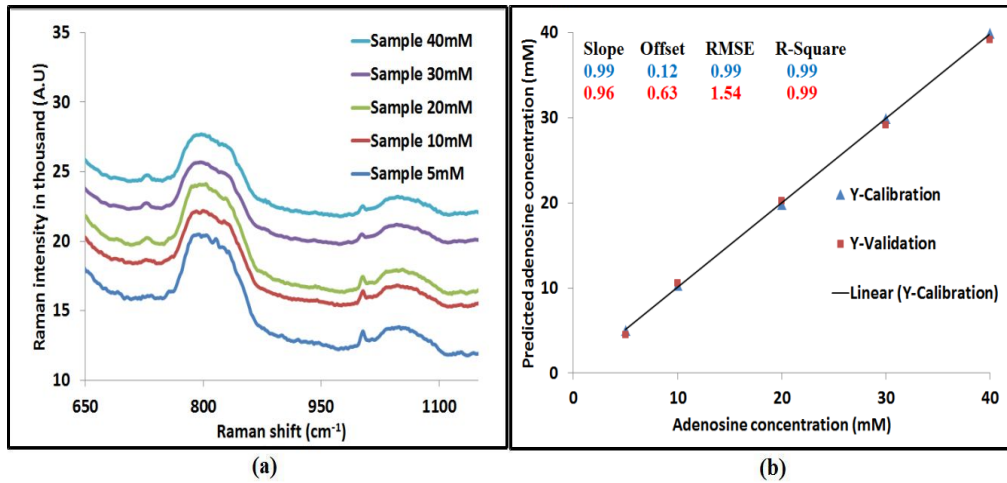


Fig. 8. (a) Raman spectra of different concentration of adenosine in serum filled in a HC-PCF
(b) PLS prediction

4. Conclusion

The present work shows that integrating pressure-driven flow with a HC-PCF improves the stability, the speed of filling and the reusability of HC-PCFs, and thus paves the path for a HC-PCF based Raman sensing platform to be utilized for real-time monitoring and diagnostic applications. We found that a pressure difference of 60psi across the HC-PCF enabled the filling of sample into a HC-PCF of length 10cm within 4min. The experimentally measured filling/draining times for samples into the HC-PCF corresponded closely to their expected values. The filling time can further be reduced by increasing the pressure difference or by decreasing the length of the fiber. The spectral reproducibility for various cycles of sample injection into HC-PCF was also verified. Our experimental configuration allowed complete filling of samples into HC-PCF which was consistent for all sets of sample mixtures. For the first time, it ensured stable operation of the HC-PCF based Raman sensor, resulting in high

quality spectral data. With the achievement of stability and reproducibility of the Raman spectra by integrated HC-PCF pressure driven system, we have demonstrated the application of partial least square (PLS) analysis on the spectral data to accurately predict the concentration of ethanol, isopropanol, heparin and adenosine in the sample mixture. The present detection scheme has immense potential for high sensitivity, rapid real-time monitoring of various concentrations of chemical species that are of clinical and environmental importance.